

Nonlinear Model-based Position Control for Quadrotor UAVs

Marius Beul, University of Bonn, mbeul@ais.uni-bonn.de, Germany
Rainer Worst, Fraunhofer IAIS, rainer.worst@iais.fraunhofer.de, Germany
Sven Behnke, University of Bonn, behnke@cs.uni-bonn.de, Germany

Abstract

Position control of Micro Air Vehicles (MAV) is challenging, because position measurements by global navigation satellite systems or laser scanners are typically available at much lower rates than the control frequency. Furthermore, the transient response of classic PID controllers is either slow or induces overshoot. In this work, we address this issue by a model-based control approach. We model and identify the dynamics of the MAV and use this knowledge in a nonlinear cascaded controller to generate time-optimal trajectories. The proposed method is evaluated in simulation and two real MAVs.

Keywords: Position control, Model based control, MAV, UAV, Quadrotor

1 Introduction

In recent years, micro aerial vehicles (MAVs) have become widely available. Due to their low cost and flexibility, they are used for aerial photography, inspection, surveillance and rescue missions.

In most cases, a human operator pilots the MAV remotely to fulfill a specific task or the MAV is following a predefined path of GPS waypoints in an obstacle-free altitude. Instead of remotely operating the MAV, we aim for a fully autonomous flight.

For the above mentioned tasks, a high level of autonomy is necessary, including the capability of flying to and staying at waypoints. To this end, a model-based position controller is developed in this work. Particular attention is needed in terms of overshoot and settling time of the controller. During missions in restricted environments such as urban areas with close-to-wall flying, overshoot could easily lead to collisions. Time is also a crucial asset in these operations, since the battery strictly limits the achievable flight time. Section 2 briefly describes the MAVs used in this work.

2 Micro Aerial Vehicles

2.1 MAV 1

Successful execution of rescue operations demand quick response from the fire-fighters which may cause physical and psychological stress on them during emergency services. In order to facilitate them to perform their task efficiently, a MAV (**Fig. 1**) is developed to support such operations. The MAV serves as a mobile sensor platform and operates in coopera-

tion with the humans involved. For a comprehensive specification of the MAV properties see [1]. The setup can be summarized as follows:

Sensors:

- 1× 2D Laser scanner
- 1× GPS
- 1× Inertial measurement unit (IMU)
- 1× Camera dome

Processing:

- 1× Intel-Atom 1.6 GHz
- 1× Mikrokopter FlightCtrl

Actuators:

- 8× Coaxial Robbe ROXXY 2827-35



Figure 1: MAV with GPS, laser scanner and camera dome used in rescue operations

2.2 MAV 2

Furthermore, we create mission-specific semantic maps on demand. Special focus lies on the inspection of a building’s facade [2]. Hence, the MAV has to operate in the vicinity of buildings and other structures, e.g. trees and power cables. For this purpose, a planning algorithm generates optimal paths through the previously mapped environment (**Fig. 2**). Further information on planning is found in [3].

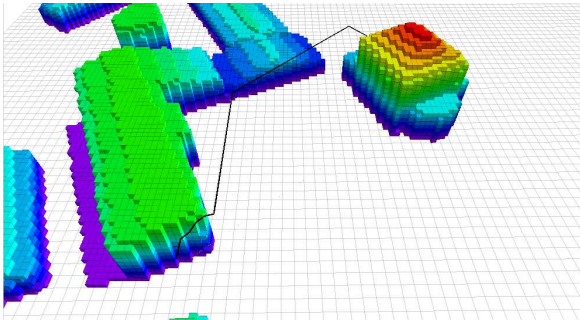


Figure 2: Map of the surroundings of the MAV with planned trajectory

Our MAV used for these tasks is shown in **Fig. 3**. It is equipped with a variety of sensors with complimentary properties.



Figure 3: MAV equipped with DGPS, stereo cameras and 3D laser scanner

For a detailed description of our sensor setup and the processing pipeline see [4, 5, 6]. The setup can be summarized as follows:

Sensors:

- 2× Fisheye stereo cameras
- 1× 3D laser scanner (rotating 2D scanner)
- 1× Motion camera [7]
- 1× Differential GPS (DGPS) [8]
- 1× Inertial measurement unit (IMU)
- 8× Ultrasonic distance sensors

Processing:

- 1× Intel Core i7 3820QM 2.7 GHz
- 1× Pixhawk Autopilot

Actuators:

- 8× Coaxial MK3638 Motors

3 Related Work

Most traditional position controllers are based on standard proportional-integral-derivative (PID) controllers. Commercially available platforms like the Mikrokopter, the PX4 or the OpenPilot CopterControl use linear PID-controllers for positioning.

Li et al. [9] and R. Baránek et al. [10] create a dynamic model of a quadrotor. Positioning is also achieved with classic PID-control based on parameters obtained from simulation. Puls et al. [11] describe a PI-controlled quadrotor. It relies on a dynamic model and is enhanced with a correction term to lead the quadrotor on a straight path to the target. A linear state-space model is identified and parameterized by Pfeifer et al. [12]. Subsequently, a linear state-space controller is implemented and parameterized via pole placement. Bouabdallah et al. [13] derive a model from differential equations. Basic PID and backstepping control techniques are combined to control attitude, height, and position of the quadrotor. A nonlinear model of a MAV is created by Patel et al. [14]. It consists of a linear and a nonlinear part which are controlled separately by PID and sliding mode control. Some works employ machine learning techniques for quadrotor control. Dierks et al. [15], for example, use neural networks to learn the quadrotor dynamics and for positioning. All approaches have in common, that multiple parameters and gains have to be adjusted. Either simple PID gains or complex model parameters have to be found to achieve a good transient response. In this work, a model with very few physically meaningful parameters is derived, which is identified and used for model-based control.

4 Modeling MAV Dynamics

4.1 Physics-based Model

A grey-box model of the 2D-dynamics of the MAV is developed. It is assumed that the MAV is symmetrical

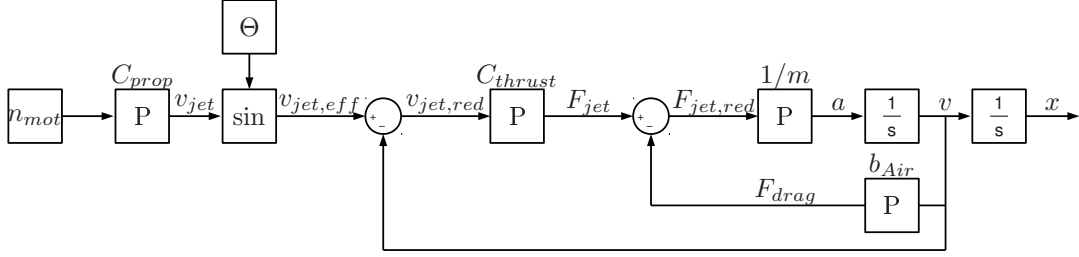


Figure 4: Grey-box model of the 1D-kinematics of the MAV with two DoF.

and thus can be modelled as a superposition of two identical models with two degrees of freedom (DoF) each (deflection Θ and position x). It is also assumed that the MAV is equipped with an underlying attitude and an overlying height controller. Considering differential equations of motion, **Fig. 4** shows an approach for the model. The MAV is modeled as point mass with state variables $[v, x]$ (velocity and position).

Assuming the MAV is hovering at constant height, the rotation speed of all motors n_{mot} results in a constant jet stream v_{jet} . This is represented by constant C_{prop} , which depends on aerodynamic properties of the propellers. The direction of the jet stream is governed by the deflection of plant input Θ . The resulting jet $v_{jet,eff}$ is reduced by the movement of the MAV v and amplified by the thrust constant C_{thrust} . This constant represents the size of the jet stream and the aerodynamic properties of the MAV. Reduced by the drag and concerning the mass of the MAV, this force propels the MAV with acceleration a which results in the velocity v and furthermore in the movement x of the MAV.

With the following restrictions made, the model can be massively simplified to the double integrator shown in **Fig. 5**.

- Small angular deflection ($\sin(v_{jet}) \approx v_{jet}$)
- Slow horizontal movement ($v_{jet,eff} \gg v$)
- Constant height ($n_{mot} \approx const.$)
- Negligibly small drag ($F_{jet} \gg F_{drag}$)

The plant input Θ is amplified with the model specific gain C_{acc} , which results in the acceleration a of the MAV that is integrated to the velocity v and the movement x .

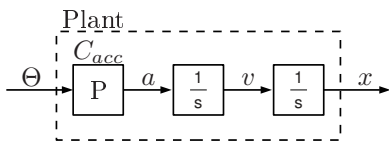


Figure 5: Simplified grey-box model of the 1D-kinematics of the MAV with two DoF.

4.2 Parameter Identification

The model is fitted with experimental data. For this model only one parameter has to be identified. This is done by fitting the MAV model with experimental data obtained in various test flights using gradient descend. For our MAVs, equations 1 to 3 hold;

$$C_{acc} = \frac{C_{prop} C_{thrust} n_{motor}}{m}, \quad (1)$$

$$C_{acc, MAV1} = 9.3 \frac{m}{s^2}, \quad (2)$$

$$C_{acc, MAV2} = 8.5 \frac{m}{s^2}. \quad (3)$$

5 Model-based Control

Based on the identified model, a nonlinear controller is developed (**Fig. 6**). We limit the allowed deflection of the MAV in order to avoid high-speed or dynamic flight maneuvers, which could be dangerous in the vicinity of obstacles. Large deflections would also prevent the linearization of the model in Fig. 5. Despite these precautions, overshoot is not permissible as it could lead to collisions during close-to-wall flying.

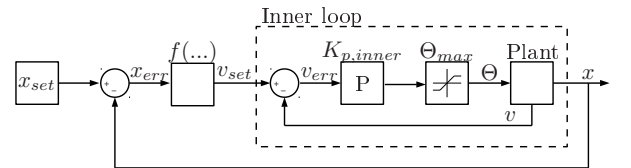


Figure 6: Closed loop control structure.

It can be seen that a cascaded control loop is used to control the position x as well as the velocity v of the MAV.

The inner loop consists of a P-controller which set-point is driven by an outer loop. Although the outer loop could also be a P-controller to archive perfect transient responses (infinitely small settling time without overshoot) in a non-limited system, here the outer loop has to be nonlinear.

Considering simple equations of motion, Eq. 4 shows

the nonlinear part of the controller $f(\dots)$. With respect to the limited plant input, this controller is capable of achieving time-optimal responses without the handicap of adjusting multiple gains:

$$f(\dots) = \sqrt{2 \frac{\Theta_{max} \cdot C_{acc}}{x_{err}}} . \quad (4)$$

Since both axes are controlled separately, the resulting trajectory to the target is bowed. This behavior is shown in **Fig. 7**.

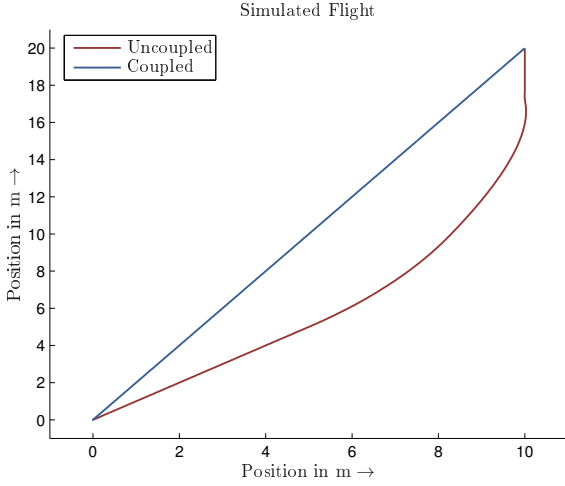


Figure 7: Flight trajectory with decoupled and coupled axes ($x_{start} = [0\text{ m}, 0\text{ m}]$, $x_{stop} = [10\text{ m}, 20\text{ m}]$, $\Theta_{max} = 5^\circ$, $C_{acc} = 9.3 \frac{\text{m}}{\text{s}^2}$, $K_{p,inner} = 10 \frac{\text{s}}{\text{m}}$).

This issue is addressed by defining a master, and a slave axis, following the idea proposed for example in [16]. Both axes predict the time of arrival on the next waypoint from the current state. This is done analytically by solving Eq. 5 to Eq. 8.

$$\int v dt = x_{err} \quad (5)$$

$$\int v dt = vt_{acc} + \frac{1}{2}v_{max}t_{dec} + \frac{1}{2}(v_{max} - v)t_{acc} \quad (6)$$

$$v_{max} = v + t_{acc}\Theta_{max}C_{acc} \quad (7)$$

$$t = t_{acc} + t_{dec} \quad (8)$$

The solution is

$$t = -\frac{v}{\Theta_{max}C_{acc}} + \sqrt{\frac{v^2}{2 \cdot (\Theta_{max}C_{acc})^2} + \frac{x_{err}}{\Theta_{max}C_{acc}}} .$$

The master is defined as the axis with the higher time of arrival. Subsequently Θ_{max} of the slave axis is set to match the arrival time:

$$\Theta_{max,sl} = \frac{-\frac{v_{sl}}{t_{ma}} + \frac{2x_{sl}}{t_{ma}^2} + \sqrt{(\frac{v_{sl}}{t_{ma}} - \frac{2x_{sl}}{t_{ma}^2})^2 + \frac{v_{sl}^2}{t_{ma}^2}}}{C_{acc}} .$$

6 Experiments

The algorithm is first implemented and evaluated in simulation (Section 6.1). In Section 6.2, it is applied and evaluated on the MAV.

6.1 Simulation

Fig. 8 shows the simulated step response and subsequent position hold.

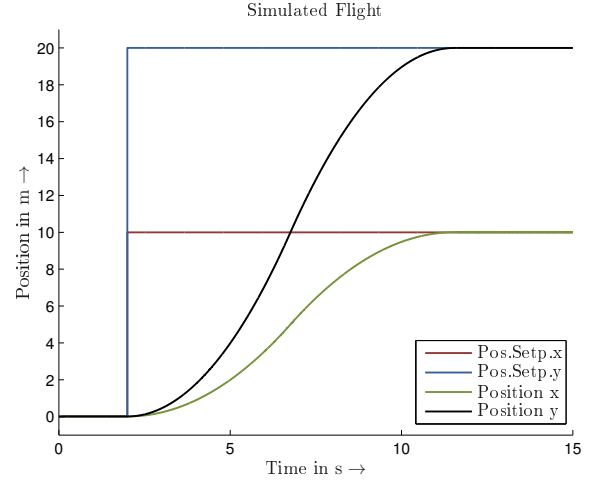


Figure 8: Step response in simulation ($x_{start} = [0\text{ m}, 0\text{ m}]$, $x_{stop} = [10\text{ m}, 20\text{ m}]$, $\Theta_{max} = 5^\circ$, $C_{acc} = 9.3 \frac{\text{m}}{\text{s}^2}$, $K_{p,inner} = 10 \frac{\text{s}}{\text{m}}$).

The feedback for the controller in simulation contains no noise and has an update rate of 1 kHz. The coupled behavior is also shown in Fig. 7. **Fig. 9** shows the corresponding velocity trajectories.

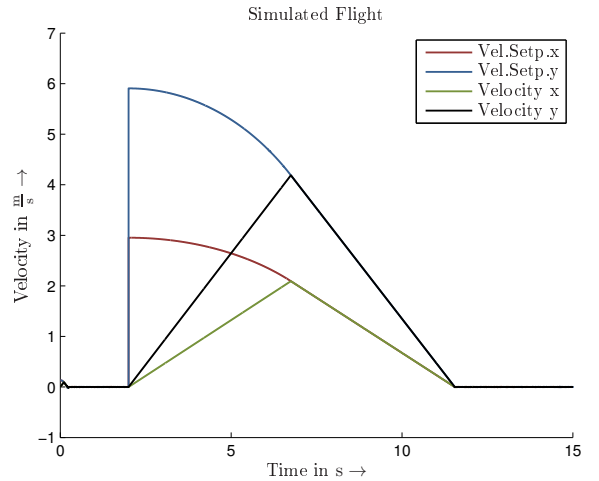


Figure 9: Step response in simulation ($x_{start} = [0\text{ m}, 0\text{ m}]$, $x_{stop} = [10\text{ m}, 20\text{ m}]$, $\Theta_{max} = 5^\circ$, $C_{acc} = 9.3 \frac{\text{m}}{\text{s}^2}$, $K_{p,inner} = 10 \frac{\text{s}}{\text{m}}$).

As can be seen in Fig. 8, these profiles lead to exact positioning in both axes at the same time. By limiting

the deflection of the slave axis, an unbowed yet time optimal trajectory is generated.

6.2 Real MAV Flight

The control algorithm is also evaluated in real MAV-flight. **Fig. 10** shows a transient response, recorded with MAV 1.

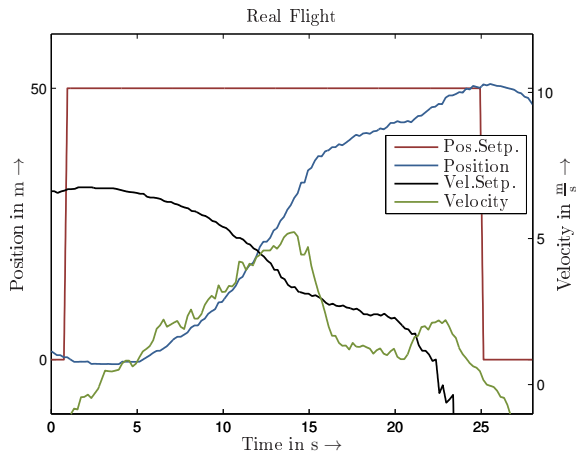


Figure 10: Step response ($x_{start} = 0$ m, $x_{stop} = 50$ m, $\Theta_{max} = 3^\circ$, $C_{acc} = 9.3 \frac{m}{s^2}$, $K_{p,inner} = 10 \frac{s}{m}$).

It can be seen that the feedback provided by the on-board GPS is much less accurate than the simulated feedback. It leads to overshoot in the velocity. Nevertheless, the overshoot in the position is negligibly small. Furthermore, it can be seen that for example at $t = 12$ s – 16 s, the measured velocity decreases faster than the planned velocity profile. This is an indication for modelling uncertainties.

The algorithm is compared to the existing Mikrokopter position controller. **Table 1** shows the results.

Controller	Θ_{max}	Settling Time	Overshoot
Nonlinear	2°	45 s	1.3 m
Nonlinear	3°	18 s	0.7 m
Nonlinear	5°	14 s	3.3 m
Mikrokopter	-	18 s	2.2 m

Table 1: Performance of the controller

It can be seen that even with bad feedback (no DGPS available) and error-prone parameterization the nonlinear approach shows better results than the original controller. For this very feedback (GPS with 5 Hz) and model parameterization, a maximum deflection of $\Theta_{max} = 3^\circ$ would be recommended.

7 Conclusions

In this paper, an approach for a model-based position controller for an unmanned MAV was presented.

A simplified model is derived from differential equations. Model parameters are fitted to the real system to approximate the MAV dynamics. A nonlinear cascaded controller, which is capable of handling the strictly limited plant input, is proposed. The control algorithm is implemented in simulation and on a real MAV. It is evaluated and compared to the existing system.

Due to the easy model identification process and the ability to reach waypoints without overshoot, the approach proposed in this paper is applicable to close-to-wall flying. The ability to stay on a linear trajectory in combination with the fast transient response make the controller ideal for MAVs with limited deflection. Since the dynamics is limited by the slow and inaccurate feedback, additional research will address this issue. Especially the use of DGPS on MAV 2 will be subject to further research. Also the ability to pass waypoints at a certain speed will be investigated. Furthermore, including height control as a third coupled axis will lead to straight paths in 3D space.

8 Acknowledgments

This research is supported by the EU FP7 ICT , Project #247870FP7 NIFTi and grant BE 2556/8 of German Research Foundation (DFG).

References

- [1] V. Tretyakov, J. Winzer and R. Worst. Platform manufacturing and sensor integration (UAV). *Fraunhofer IAIS*, 2010
- [2] S. Loch-Dehbi, Y. Dehbi and L. Plümer. Stochastic reasoning for UAV supported reconstruction of 3D building models. *ISPRS XL-1/W2*, 2013
- [3] M. Nieuwenhuisen and S. Behnke. Hierarchical Planning with 3D Local Multiresolution Obstacle Avoidance for Micro Aerial Vehicles. *ISR / Robotik*, 2014
- [4] M. Nieuwenhuisen, D. Droschel, J. Schneider, D. Holz, T. Labe, and S. Behnke. Multimodal obstacle detection and collision avoidance for micro aerial vehicles. *6th European Conference on Mobile Robots (ECMR)*, 2013
- [5] D. Droschel, J. Stuckler, and S. Behnke. Local multiresolution representation for 6D motion estimation and mapping with a continuously rotating 3D laser scanner. *IEEE International Conference on Robotics and Automation (ICRA)*, 2014

- [6] L. Klingbeil, M. Nieuwenhuisen, J. Schneider, C. Eling, D. Droeschel, D. Holz, T. Läbe, W. Förstner, S. Behnke and H. Kuhlmann. Towards Autonomous Navigation of an UAV-based Mobile Mapping System. *International Conference on Machine Control & Guidance*, 2014
- [7] D. Honegger, L. Meier, P. Tanskanen and M. Pollefeys. An open source and open hardware embedded metric optical flow CMOS camera for indoor and outdoor applications. *IEEE International Conference on Robotics and Automation (ICRA)*, 2013
- [8] C. Eling, L. Klingbeil, M. Wieland and H. Kuhlmann. A precise position and attitude determination system for lightweight unmanned aerial vehicles. *ISPRS*, 2013.
- [9] J. Li and Y. Li. Dynamic analysis and PID control for a quadrotor. *Proc. of IEEE International Conference on Mechatronics and Automation*, 2011
- [10] R. Baránek and F. Šolc. Modelling and control of a hexa-copter. *13th International Carpathian Control Conference (ICCC)*, 2012
- [11] T. Puls, M. Kemper, R. Küke and A. Hein. GPS-based position control and waypoint navigation system for quadcopters. *International Conference on Intelligent Robots and Systems*, 2009
- [12] E. Pfeifer, F. Kassab Jr. Dynamic feedback controller of an unmanned aerial vehicle. *Brazilian Robotics Symposium and Latin American Robotics Symposium*, 2012
- [13] S. Bouabdallah and R. Siegwart. Full control of a quadrotor. *Proceedings of the IEEE/RSJ IROS*, 2007
- [14] A. R. Patel, M. A. Patel and D. R. Vyas. Modeling and analysis of quadrotor using sliding mode control. *44th IEEE Southeastern Symposium on System Theory*, 2012
- [15] T. Dierks and S. Jagannathan. Output feedback control of a quadrotor UAV using neural networks. *IEEE Transactions on Neural Networks*, 2010.
- [16] D. A. Pierre. Optimization Theory with Applications. *Dover Publications*, 1986